



## Material properties and modeling characteristics for MnFeP<sub>1-x</sub>As<sub>x</sub> materials for application in magnetic refrigeration

Engelbrecht, Kurt; Nielsen, Kaspar Kirstein; Bahl, Christian R.H.; Carroll, C. P.; van Asten, D.

*Published in:*  
Journal of Applied Physics

*Link to article, DOI:*  
[10.1063/1.4803495](https://doi.org/10.1063/1.4803495)

*Publication date:*  
2013

*Document Version*  
Publisher's PDF, also known as Version of record

[Link back to DTU Orbit](#)

*Citation (APA):*  
Engelbrecht, K., Nielsen, K. K., Bahl, C. R. H., Carroll, C. P., & van Asten, D. (2013). Material properties and modeling characteristics for MnFeP<sub>1-x</sub>As<sub>x</sub> materials for application in magnetic refrigeration. *Journal of Applied Physics*, 113(17), 173510. <https://doi.org/10.1063/1.4803495>

---

### General rights

Copyright and moral rights for the publications made accessible in the public portal are retained by the authors and/or other copyright owners and it is a condition of accessing publications that users recognise and abide by the legal requirements associated with these rights.

- Users may download and print one copy of any publication from the public portal for the purpose of private study or research.
- You may not further distribute the material or use it for any profit-making activity or commercial gain
- You may freely distribute the URL identifying the publication in the public portal

If you believe that this document breaches copyright please contact us providing details, and we will remove access to the work immediately and investigate your claim.

## Material properties and modeling characteristics for MnFeP<sub>1-x</sub>As<sub>x</sub> materials for application in magnetic refrigeration

K. Engelbrecht, K. K. Nielsen, C. R. H. Bahl, C. P. Carroll, and D. van Asten

Citation: *J. Appl. Phys.* **113**, 173510 (2013); doi: 10.1063/1.4803495

View online: <http://dx.doi.org/10.1063/1.4803495>

View Table of Contents: <http://jap.aip.org/resource/1/JAPIAU/v113/i17>

Published by the [American Institute of Physics](#).

---

### Additional information on *J. Appl. Phys.*

Journal Homepage: <http://jap.aip.org/>

Journal Information: [http://jap.aip.org/about/about\\_the\\_journal](http://jap.aip.org/about/about_the_journal)

Top downloads: [http://jap.aip.org/features/most\\_downloaded](http://jap.aip.org/features/most_downloaded)

Information for Authors: <http://jap.aip.org/authors>

## ADVERTISEMENT



The advertisement banner features a green and white background with abstract, flowing lines. On the left, the text 'AIP Advances' is displayed in a green, sans-serif font, with a series of orange and yellow circles of varying sizes arranged in an arc above the word 'Advances'. On the right, there is a circular seal with a white border containing the text 'Now Indexed in Thomson Reuters Databases'. Below this, a dark blue horizontal bar contains the text 'Explore AIP's open access journal:' in white, followed by a list of three bullet points in white text.

**AIP Advances**

Now Indexed in  
Thomson Reuters  
Databases

Explore AIP's open access journal:

- Rapid publication
- Article-level metrics
- Post-publication rating and commenting

# Material properties and modeling characteristics for $\text{MnFeP}_{1-x}\text{As}_x$ materials for application in magnetic refrigeration

K. Engelbrecht,<sup>1,a)</sup> K. K. Nielsen,<sup>1</sup> C. R. H. Bahl,<sup>1</sup> C. P. Carroll,<sup>2</sup> and D. van Asten<sup>3</sup>

<sup>1</sup>*DTU Energy Conversion and Storage, Technical University of Denmark, Frederiksborgvej 399, DK-4000 Roskilde, Denmark*

<sup>2</sup>*BASF Future Business GmbH, 4. Gartenweg, 67063 Ludwigshafen, Germany*

<sup>3</sup>*BASF Nederland BV, Strijkviertel 67, 3454 De Meern, Holland*

(Received 27 February 2013; accepted 12 April 2013; published online 6 May 2013)

Compounds of  $\text{MnFeP}_{1-x}\text{As}_x$  have received attention recently for their use in active magnetic regenerators (AMR) because of their relatively high isothermal entropy change and adiabatic temperature change with magnetization. However, the materials also generally exhibit a significant magnetic and thermal hysteresis, and it is not well understood how the hysteresis will affect performance in a practical AMR device. The amount of hysteresis shown by a material can be controlled to an extent by tuning the processing conditions used during material synthesis; therefore, knowledge of the practical impact of hysteresis is a key element to guide successful material development and synthesis. The properties of a magnetocaloric  $\text{MnFeP}_{1-x}\text{As}_x$  compound are characterized as a function of temperature and applied magnetic field, and the results are used to assess the effects of hysteresis on magnetocaloric properties. Different methods of building property functions from the measured specific heat, magnetization, and adiabatic temperature change are presented. It is shown that model predictions can be highly dependent on how the properties that are used by the AMR model are calculated. © 2013 AIP Publishing LLC.

[<http://dx.doi.org/10.1063/1.4803495>]

## I. INTRODUCTION

Active magnetic regenerative (AMR) refrigerators are a potentially environmentally friendly alternative to vapor compression technology that may be used for air-conditioning, refrigeration, and heat pump applications. Rather than using a gaseous refrigerant, AMRs use solid magnetocaloric materials (MCM) that have a coupling between their thermodynamic properties and internal magnetic field. Assuming the material properties are independent of pressure, the entropy,  $s$ , of a magnetocaloric material can be expressed on differential form as

$$ds = \frac{c_H}{T} dT + \left( \frac{\partial s}{\partial H} \right)_T dH, \quad (1)$$

where  $H$  is the magnetic field,  $T$  is temperature, and  $c_H$  is the specific heat at constant magnetic field. As the magnetic field is increased, the entropy of a magnetocaloric ferromagnetic material decreases as it moves to a magnetically more ordered state. Equation (1) illustrates that the temperature of the material must increase when the material is magnetized adiabatically to maintain constant entropy since  $\frac{\partial s}{\partial H} < 0$ . The magnitude of the temperature increase is related to the specific heat and the magnetic entropy change with magnetization of the material. This coupling between magnetic field and temperature allows thermodynamic cycles that can accept a cooling load and reject it to a thermal reservoir with a higher temperature when magnetic work is applied to the system.

The first regenerative magnetic refrigeration device used a superconducting electromagnet and demonstrated that a regenerator cycle could accept a cooling load at a much larger temperature span than the adiabatic temperature change with magnetization ( $\Delta T_{\text{ad}}$ ) of the material.<sup>1</sup> Since then, many new devices have been reported,<sup>2</sup> with the most recent research focused on permanent magnet devices. The majority of experimental devices reported use gadolinium and its alloys as the solid refrigerant; however, developing and characterizing new MCMs is an active research topic and the properties of many new compositions are reported each year.<sup>3</sup> One material series that is being considered as a potential high-performance MCM is  $\text{MnFeP}_{1-x}\text{As}_x$  because the materials exhibit high entropy change with magnetization,  $\Delta s_{\text{mag}}$ , and high  $\Delta T_{\text{ad}}$ . The materials are also attractive because they do not contain rare earth compounds and may be relatively inexpensive to produce. The properties and processing of these materials are well known and have been reported by Refs. 4–6. The Curie temperature of these materials can be modified by substituting P for As to achieve Curie temperatures from below 200 K to greater than 330 K. The materials generally undergo a first order magnetic phase transition<sup>5</sup> and there is generally some hysteresis observed in these materials. Although hysteresis values have been quantified on this series of materials, there has been little investigation into how this hysteresis affects the material's magnetocaloric properties when utilized in an AMR. In this paper, measurements of the magnetocaloric properties of a  $\text{MnFeP}_{1-x}\text{As}_x$  compound are presented. The characterization includes redundant property measurements that are used to confirm how hysteresis affects the magnetocaloric properties and a method to build property functions that can be used by

<sup>a)</sup>Email: kuen@risoe.dtu.dk

numerical AMR models of regenerators using  $\text{MnFeP}_{1-x}\text{As}_x$  compounds to a first approximation is suggested.

Recently, more attention has been paid to hysteresis effects in magnetocaloric materials. The hysteresis of MnAs was studied,<sup>7</sup> and it was found that the magnetocaloric properties were highly dependent on the material's history. A separate study of MnAs showed that the material exhibited no  $\Delta T_{\text{ad}}$  when the magnetic field was below 2.5 T.<sup>8</sup> The authors concluded that the magnetocaloric effect is wiped out by hysteresis at lower magnetic fields. It was recently shown experimentally that hysteresis reduces  $\Delta T_{\text{ad}}$  in  $\text{La}(\text{Fe},\text{Si})_{13}$  compounds.<sup>9</sup> The effect of hysteresis on the AMR cycle has been studied using non-equilibrium thermodynamics and shown to reduce the cooling power in an AMR.<sup>10</sup>

## II. MATERIAL PREPARATION

A magnetocaloric composition of  $\text{MnFeP}_{1-x}\text{As}_x$  was produced by first milling elementary Mn, Fe, P, and As in a high-intensity mill. Fine powders were obtained which were compacted at 4000 bars in a cold isostatic press. These pressed bodies were then sintered at 1273 K under argon atmosphere and subsequently annealed at 923 K. Further details on the synthesis can be found in Ref. 11.

## III. MATERIAL CHARACTERIZATION

### A. Magnetocaloric properties

The magnetocaloric properties of the  $\text{MnFeP}_{1-x}\text{As}_x$  material in the sintered state were measured using a differential scanning calorimeter (DSC) to measure specific heat, a vibrating sample magnetometer (VSM) to measure magnetization, and an adiabatic magnetization device to directly measure the adiabatic temperature change with magnetization. The DSC is described in detail in Ref. 12. The VSM is a commercial LakeShore 7407 device, and the adiabatic magnetization device is custom-built and described in Ref. 13.

The applied field may, in all three devices, be varied between 0 and 1.5 T. The temperature range of the DSC is 230–320 K; in the VSM, it is 80–450 K and in the adiabatic temperature change device, it is 255–310 K. The differential scanning calorimetry was done at a temperature ramp rate of 1 K/s, which has been found to be a good compromise between having an acceptable signal to noise ratio, keeping the experiment runtime around 4 h and ensuring a minimum temperature lag in the sample. The sample was measured both while heating (from 230 to 320 K) and cooling (from 320 to 230 K) at applied fields of 0, 0.5, 1.0, and 1.5 T, respectively.

The magnetometry was performed at constant applied fields of 0.005, 0.25, 0.5, 0.75, 1.0, 1.25, and 1.5 T, respectively, for both heating and cooling between 270 and 310 K in discrete steps of 1 K. Each data point was obtained after 5 min at the requested temperature to ensure thermodynamic equilibrium and the applicability of the appropriate Maxwell relation so that the magnetic entropy change may be calculated.

The adiabatic temperature change was measured from 0 T to applied fields of 1.0 and 1.5 T. The experiments started with the system at an equilibrium temperature of 255 K, and the temperature was then slowly ramped to 310 K in about

5 h for each applied field. The sample temperature was measured with a thermocouple (type E, i.e., non-magnetic) that was fixed to the sample with thermally conducting glue. The sample rate was 5 Hz while application/removal of the applied field takes approximately 1 s, which ensures that the magnetization and demagnetization processes were sufficiently resolved in the experiment.

### B. Peak temperatures and hysteresis

Since the Curie temperature of first order materials that exhibit hysteresis is not straightforward to define, the material here is defined by the temperature where the maximum  $\Delta T_{\text{ad}}$  when magnetized from 0 T to 1.5 T is observed. The value is defined as  $T_{\text{peak}}$  and is expected to be similar in value to the Curie temperature but not generally identical to it.

The specific heat was found to depend on the thermal history of the sample, meaning that there are separate curves for properties measured while heating and cooling. The specific heat measured at two different magnetic fields is plotted in Fig. 1.

The magnetization as a function of temperature was measured for several magnetic fields and was then used to calculate the isothermal entropy change,  $\Delta s_{\text{mag}}$ , with the conventional integration method. The calculated  $\Delta s_{\text{mag}}$  values are plotted in Fig. 2. The adiabatic temperature change was directly measured and the results are summarized in Fig. 3. The adiabatic temperature change device measures the change in temperature of the material as it is both magnetized and demagnetized, resulting in two different curves. The data can therefore be checked to ensure that the material returns to its original temperature when it is magnetized then demagnetized adiabatically, meaning it undergoes a reversible magnetocaloric effect. The results showed that the magnetocaloric effect was found to be reversible within experimental uncertainty over the entire temperature range that was measured. This is an important result, as it means that the material undergoes a reversible magnetocaloric effect under dynamic conditions, although it exhibits hysteresis in the specific heat and entropy change measurements that were performed.

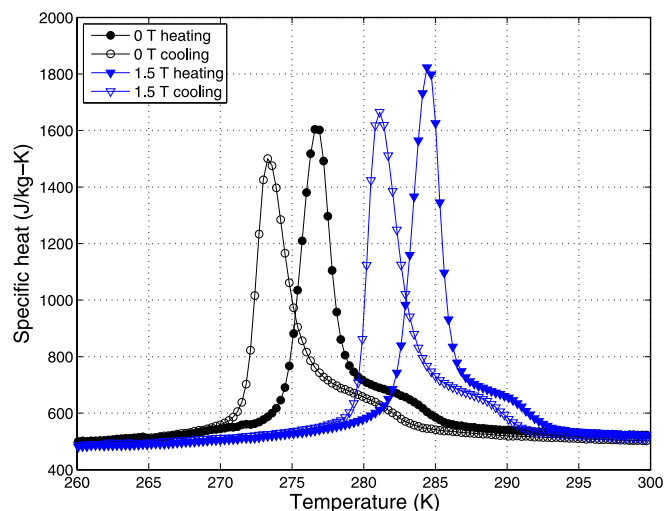


FIG. 1. Specific heat measurement using a DSC at 0 T and 1.5 T for cooling (open symbols) and heating (filled symbols).

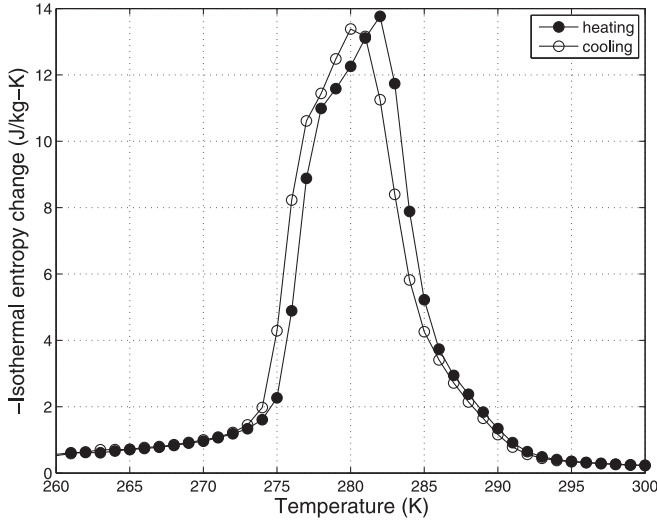


FIG. 2. The absolute isothermal entropy change when magnetized from 0 T to 1.5 T for cooling (open symbols) and heating (filled symbols).

The measured value of  $T_{\text{peak}}$  was 278.1 K,  $\Delta T_{\text{ad,max}}$  is 3.1 K and  $c_{\text{max,0T}}$  is 1617 J/kg-K. There are two measures of hysteresis that can be calculated from properties measured in this study: magnetization and specific heat. The magnetization is calculated as the maximum difference between the magnetization curves for cooling and heating, respectively. The specific heat hysteresis is defined as the temperature difference between the peak specific heat for heating and cooling measurements in zero field. Magnetization hysteresis is 0.5 K and the specific heat hysteresis is 3.9 K.

### C. Thermodynamic analysis

The goal of the material characterization for this article is to obtain magnetocaloric data that can be used by a numerical AMR model to predict the performance of a  $\text{MnFeP}_{1-x}\text{As}_x$  regenerator. The properties of interest are the specific heat at constant magnetic field,  $\Delta T_{\text{ad}}$  and  $\Delta s_{\text{mag}}$ , which are coupled through the entropy curves. The magnetocaloric properties of a material can be calculated from the entropy curves at

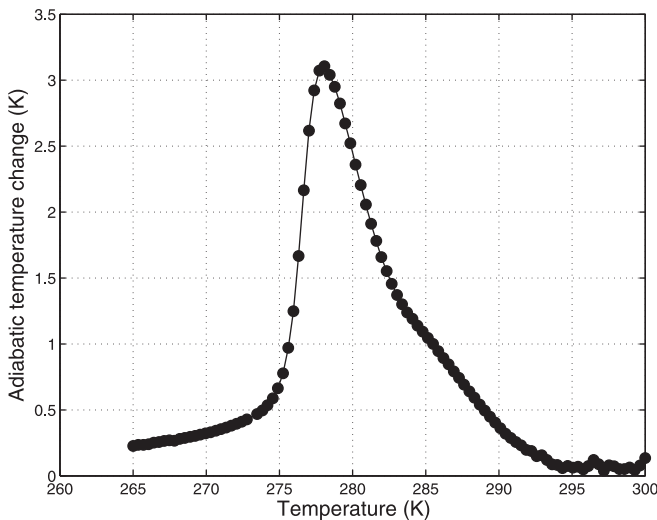


FIG. 3. The measured adiabatic temperature change when magnetized from 0 T to 1.5 T.

different magnetic fields. Assuming the MCM properties are independent of pressure, the zero-field entropy of the material can be calculated by integrating the assumed zero field specific heat

$$s(T, H = 0) = \int_{T_{\text{ref}}}^T \frac{c_{H=0}}{T'} dT', \quad (2)$$

where  $T_{\text{ref}}$  is the zero field entropy reference temperature. To calculate the entropy as a function of temperature at other fields, the following equation is used:

$$s(T, \mu_0 H) = \int_{T_{\text{ref}}}^T \frac{c_H}{T'} dT' + \Delta s_{\text{mag}}(T = T_{\text{ref}}, \mu_0 H). \quad (3)$$

The entropy curves calculated from specific heat data are plotted in Fig. 4. The entropy curves in field can also be calculated by shifting the zero field entropy along the temperature axis by  $\Delta T_{\text{ad}}$  or shifting the zero field entropy curve along the entropy axis by  $\Delta s_{\text{mag}}$ . The measured in-field specific heat,  $\Delta T_{\text{ad}}$  and  $\Delta s_{\text{mag}}$  values are therefore redundant and can be used to check the accuracy and consistency of the other measurements.

Because hysteresis is present to some degree in the material, it is not clear which specific heat or magnetization curve to use when calculating magnetization processes that move from one magnetic field to another. At each magnetic field, there is a distinct heating and cooling curve for both magnetization and specific heat. This gives four possible combinations of curves to use when calculating either  $\Delta T_{\text{ad}}$  or  $\Delta s_{\text{mag}}$  when magnetized from 0 to 1.5 T. As illustrated in Fig. 4, the combinations are: the cooling curve in zero field and cooling curve in high field (cool-cool); the cooling curve in zero field and heating curve in high field (cool-heat); the heating curve in zero field and cooling curve in high field (heat-cool); and the heating curve in zero field and heating curve in high field (heat-heat).

The first check of property data presented here is to use the specific heat curves to calculate the  $\Delta s_{\text{mag}}$  curves and

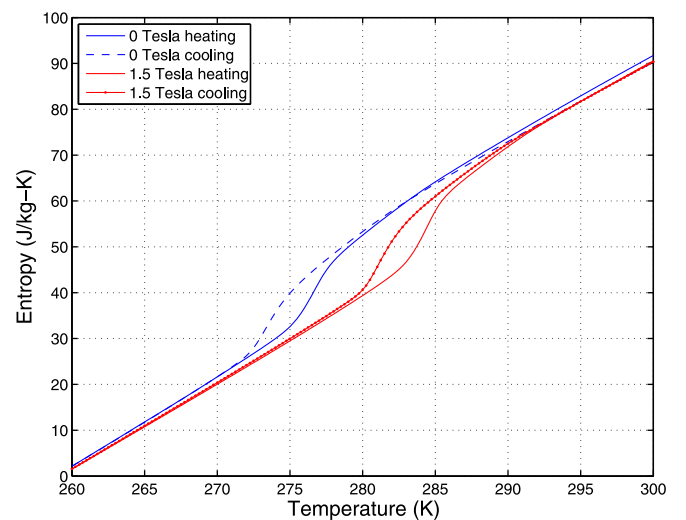


FIG. 4. The entropy at 0 T and 1.5 T for the material for both cooling and heating.

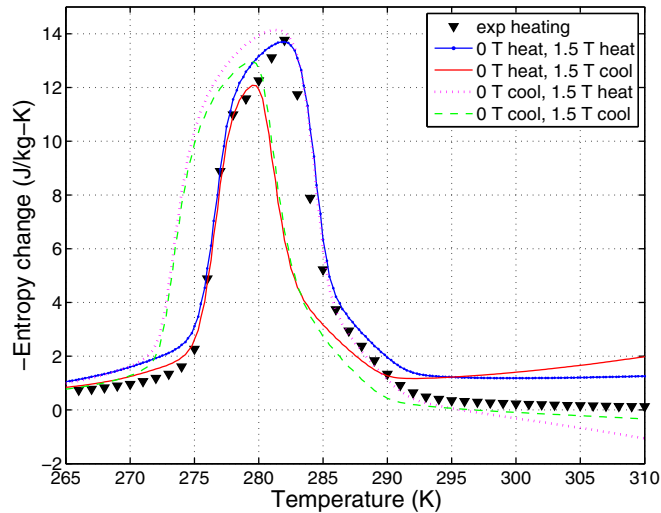


FIG. 5. The isothermal entropy change with magnetization using four combinations of specific heat measurement values compared to direct measurements for heating.

then compare them to data obtained from magnetometry. The values of  $\Delta s_{\text{mag}}$  were calculated using the four possible combinations of heating and cooling curves measured for specific heat that are mentioned above, and they are compared to data measured on the VSM in Fig. 5.

When we consider the magnetocaloric cycle, the magnetocaloric material is predominantly heating up during the low field phase, and predominantly cooling down during the high field phase. It is thus relatively logical to expect that the (heat-cool) combination might be the most physically meaningful. Indeed, in Fig. 6, the  $\Delta T_{\text{ad}}$  curves calculated from the entropy diagram using the various combinations are shown, and it is seen that the (heat-cool) combination is the one that best matches with the values for  $\Delta T_{\text{ad}}$  measured directly via experiment.

The specific heat curves were then used to calculate  $\Delta T_{\text{ad}}$  and those values were compared to the values obtained by direct measurement in Fig. 6.

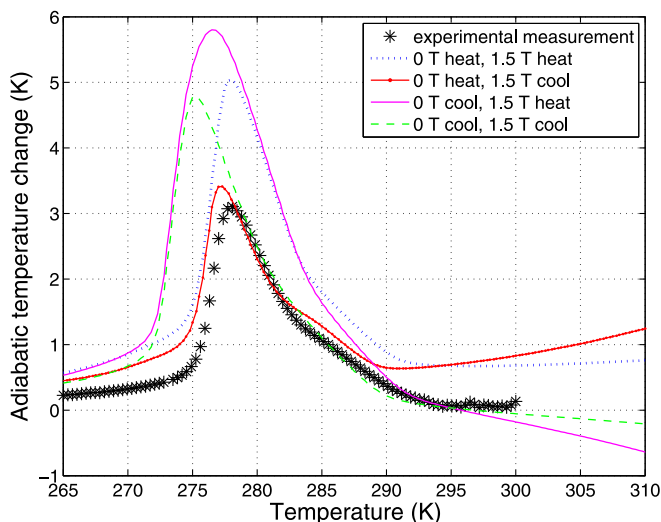


FIG. 6. The adiabatic temperature change with magnetization using four combinations of specific heat measurement values compared to direct measurements.

#### IV. MODELING OF A $\text{MnFeP}_{1-x}\text{As}_x$ REGENERATOR

In order to model a  $\text{MnFeP}_{1-x}\text{As}_x$  regenerator in a practical application, a single-regenerator AMR test machine is considered, such as that presented by Ref. 14 where the maximum magnetic field is 1.03 T. A representative regenerator size, regenerator geometry, cycle frequency, and fluid flow are chosen to illustrate the difference between using different property values for the MCM.  $T_{\text{peak}}$  of this material is assumed to be 292 K. The illustrative case is modeled using a 1D numerical AMR model described in Ref. 15. The model uses a simple technique to account for demagnetizing fields in the regenerator. The internal magnetic field is a function of the magnetization, which varies with time and location in the regenerator bed.<sup>16</sup> Accounting for the demagnetizing field directly in the AMR model adds to the numerical complexity and can greatly increase the necessary computation time.<sup>17</sup> A method used here to avoid the complexity, computation time, and increased material property data needed to precisely model the internal magnetic field in an AMR is to calculate the internal magnetic field at every spatial node in the regenerator based on an average temperature for each location using an average demagnetisation factor,  $N_{\text{avg}}$

$$\mu_0 H(x) = \frac{\mu_0 H_{\text{max}} - \mu_0 N_{\text{avg}} M(\bar{T}(x, \mu_0 H_{\text{max}}))}{\mu_0 H_{\text{max}}} \mu_0 H. \quad (4)$$

The average demagnetization factor was estimated as 0.36 for this regenerator using basic magnetostatics. The model was run using two separate data sets: one built from zero field heating and in-field heating specific heats, respectively, and the second built from zero field heating specific heat and shifting the corresponding entropy curve by the  $\Delta T_{\text{ad}}$  measured for different magnetic field changes.

#### V. DISCUSSION

The curves in Fig. 6 show that the directly measured  $\Delta T_{\text{ad}}$  values are generally closest to the combination of zero field heating and high field cooling near the  $T_{\text{peak}}$  of the material; however, it begins to deviate for temperatures far above or below  $T_{\text{peak}}$ . The direct adiabatic temperature change measurement was also shown to be reversible upon magnetization and demagnetization. Since the cyclic magnetization and demagnetization, the material experiences in the  $\Delta T_{\text{ad}}$  experiments is closer in nature to conditions experienced in an AMR device, the direct  $\Delta T_{\text{ad}}$  measurement is considered to best represent the material's magnetocaloric effect. The lower measured  $\Delta T_{\text{ad}}$  compared to those calculated from specific heat agree with earlier works<sup>8,9</sup> that hysteresis tends to reduce the magnetocaloric effect when the material is subjected to an oscillating magnetic field.

The specific heat curves agree with  $\Delta s_{\text{mag}}$  measurements when the temperature history of the material is controlled, as in the VSM measurements, within acceptable limits. This agreement suggests that the property measurements are trustworthy for the special conditions seen in the measurements but are not necessarily indicative of the properties of the

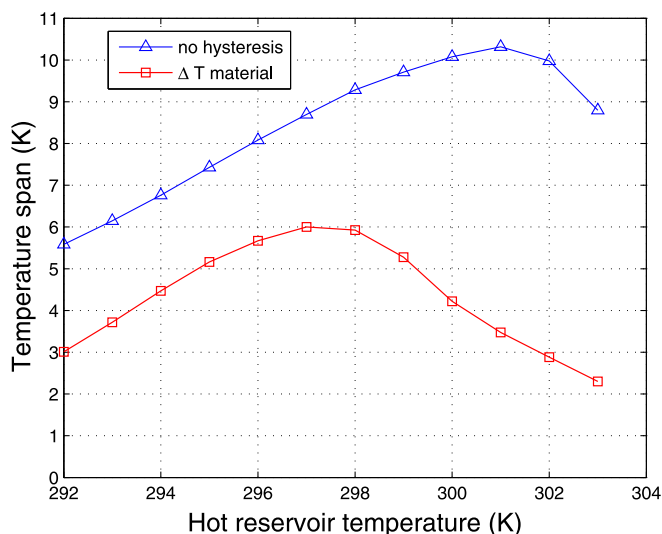


FIG. 7. Predicted no load temperature span for the  $\text{MnFeP}_{1-x}\text{As}_x$  regenerator using material properties that ignore hysteresis and materials properties built from 0 T specific heat and adiabatic temperature measurements.

material while it undergoes the AMR cycle. The specific heat measurements and comparison of material properties in Figs. 5 and 6 show that hysteresis effects can have a large influence on the magnetocaloric properties and are most likely very important to the material's performance in an AMR device. To model these materials accurately, a detailed non-equilibrium model such as that suggested by Ref. 10 combined with a detailed numerical AMR model would be required. However, this approach can greatly increase model complexity and computation time.

Using a numerical AMR model, it was shown that using material properties built using 0 T specific heat and directly measured  $\Delta T_{\text{ad}}$  values result in much more conservative predictions of AMR performance as the MCE is reduced (Fig. 7). Using properties that ignore hysteresis effects results in significantly higher predicted temperature spans for a given cooling power and a higher hot reservoir temperature where the maximum temperature span is attained. Because the direct  $\Delta T_{\text{ad}}$  measurement data more closely represent the conditions seen in an AMR, the more conservative predictions made by these material properties may be more representative of real experimental results. The modeling presented here shows that great care must be taken in determining MCM properties used in a numerical AMR model in order to obtain accurate modeling results.

## VI. CONCLUSIONS

Experimental property measurements presented here show that hysteresis in  $\text{MnFeP}_{1-x}\text{As}_x$  compounds may significantly reduce their performance in a practical AMR. It is thus essential that material hysteresis be carefully

monitored and controlled during material production. It was shown that directly measured  $\Delta T_{\text{ad}}$  is the most closely matched entropy curves that correspond to 0 field heating curves and high field cooling curves, suggesting that the material experiences the full hysteresis effect when subjected to dynamic temperature and magnetic field conditions. However, the magnetization process was shown to be reversible despite hysteresis.

Because the actual properties of  $\text{MnFeP}_{1-x}\text{As}_x$  compounds depend on the history of the material, a detailed non-equilibrium model of the compounds is necessary to accurately model these compounds. For situations when a detailed hysteresis model is either overly complex or computationally prohibitive, a simplified method to model  $\text{MnFeP}_{1-x}\text{As}_x$  compounds while still including some hysteresis effects is to build material property functions from zero field specific heat measured while heating coupled with directly measured  $\Delta T_{\text{ad}}$  data. It was shown that using this method for building MCM properties of these materials greatly influences modeling results for practical AMR operating conditions.

## ACKNOWLEDGMENTS

The financial support of BASF SE is greatly appreciated. K. K. Nielsen wishes to thank The Danish Council for Independent Research—Technology and Production Sciences (Contract No. 10-092791) for financial support.

- <sup>1</sup>G. Brown, *J. Appl. Phys.* **47**, 3673 (1976).
- <sup>2</sup>B. Yu, M. Liu, P. W. Egolf, and A. Kitanovski, *Int. J. Refrig.* **33**, 1029 (2010).
- <sup>3</sup>E. Brueck, *J. Phys. D* **38**, R381 (2005).
- <sup>4</sup>O. Tegus, E. Brueck, K. H. J. Buschow, and F. R. de Boer, *Nature* **415**, 150 (2002).
- <sup>5</sup>E. Brueck, M. Ilyn, A. M. Tishin, and O. Tegus, *J. Magn. Magn. Mater.* **290–291**, 8 (2005).
- <sup>6</sup>D. T. C. Thanh *et al.*, *J. Appl. Phys.* **103**, 07B318 (2008).
- <sup>7</sup>L. Tocado, E. Palacios, and R. Burriel, *J. Appl. Phys.* **105**, 093918 (2009).
- <sup>8</sup>L. Tocado, E. Palacios, and R. Burriel, *J. Therm. Anal. Calorim.* **84**, 213 (2006).
- <sup>9</sup>K. P. Skokov *et al.*, *J. Appl. Phys.* **111**(7), 07A910 (2012).
- <sup>10</sup>V. Basso, C. P. Sasso, G. Bertotti, and M. LoBue, *Int. J. Refrig.* **29**, 1358 (2006).
- <sup>11</sup>E. Bruck, O. Tegusi, and F. R. De Boer, "Material for magnetic refrigeration preparation and application," US patent 2004/0250550 A1 (2006).
- <sup>12</sup>S. Jeppesen, S. Linderth, N. Pryds, L. T. Kuhn, and J. B. Jensen, *Rev. Sci. Instrum.* **79**, 083901 (2008).
- <sup>13</sup>R. Bjørk, C. R. H. Bahl, and M. Katter, *J. Magn. Magn. Mater.* **322**(24), 3882 (2010).
- <sup>14</sup>K. Engelbrecht, C. R. H. Bahl, and K. K. Nielsen, *Int. J. Refrig.* **34**(4), 1132 (2011).
- <sup>15</sup>K. Engelbrecht and C. R. H. Bahl, *J. Appl. Phys.* **108**, 123918 (2010).
- <sup>16</sup>D. V. Christensen *et al.*, *J. Appl. Phys.* **108**, 063913 (2010).
- <sup>17</sup>J. Bouchard, H. Nesreddine, and N. Galanis, *Int. J. Heat Mass Transfer* **52**(5–6), 1223 (2009).